Material Defect Reconstruction by Non-Destructive Testing with Laser Induced Ultrasonics

To cite this article: H Selim *et al* 2018 *J. Phys.: Conf. Ser.* **1149** 012011

Material Defect Reconstruction by Non-Destructive Testing with Laser Induced Ultrasonics

H Selim[1], M Delgado[2], J Trull[1], R Picó[3] and C Cojocaru[1]

[1.] Universitat Politècnica de Catalunya, Physics Department, Terrassa, Barcelona, Spain
[2.] Universitat Politècnica de Catalunya, Electronic Engineering Department, Terrassa, Barcelona, Spain
[3.] Instituto de Investigación para la Gestión Integrada de Zonas Costeras, Universitat Politècnica de Valencia, Valencia, Spain

E-mail: hossam.eldin.mohamed.selim@upc.edu

Abstract. Aligned with current research efforts and industrial applications on non-destructive testing, in this work, a hybrid system combining remotely induced laser ultrasonics with conventional transducer detection is studied for defects detection in metallic parts. The processing of the induced acoustic emission waves is proposed to be approached by means of a high-resolution volumetric signal processing procedure based on the synthetic aperture focusing technique for the benefit of the final 2D visualization of the defects. The advantages of the hybrid non-destructive testing approach and the performance of the processing technique are experimentally validated.

1. Introduction

Nowadays, Non-Destructive Testing (NDT) methods are implemented in industrial applications for the detection of fractures and defects in manufactured assets and components. The most extended NDT techniques involve ultrasonic transducers for both the generation of ultrasound as well as for its detection after propagation through the material under study. The analysis is typically based on the measurement of the time of flight of ultrasonic pulses considering the distance from the emitter to the receiver, which allows the identification of discontinuities. Different configurations of this approach were extensively discussed in many research papers and applications, such as the measurement of the crack location, height and width [1–3], or of the crack penetration using bulk waves [4]. Although these methods have the advantages of low cost, and easy implementation and provide satisfactory results in many applications, the emitter transducers also show drawbacks. Some of them are the low output power that prevents such systems from being used remotely, low frequency bandwidth range that makes necessary the use of microphone arrays or ultrasonic scanners increasing the system's overall cost, small surface areas that prevent covering large object areas at once, and quite low spatial resolution in the excited volume.

As an alternative, photonic approaches based on laser induced ultrasonic and optical detection showed up as valuable competitors to the conventional ultrasonic NDT techniques, offering the possibility of remote excitation and detection at a much higher resolution [5,6]. Optical methods have important advantages such as the non-contact application, remote control and generation of broadband frequency waves (from kHz to GHz), high output power and the possibility to easily scan large object areas. The main drawbacks of optical detection methods are their high sensibility and critical stability in detection, as well as elevated costs that are acceptable only for high-resolution measurements in certain fields of application.

Considering the advantages and disadvantages of both NDT approaches, in this work, the study of a hybrid NDT scheme, where the ultrasounds are induced by laser pulses and their acquisition is done with conventional transducers, is proposed, thus, combining the main advantages of both optical and ultrasonic devices [7,8]. Laser induced ultrasound technique allows remote inspection and control, without the need of a direct contact. This technique features a broader frequency bandwidth compared with the conventional ultrasonic transducer, covering any ultrasonic bandwidth needed for various applications. It provides, then, an enhanced resolution in the excited volume and represents an easy tool for scanning the sample. On the other hand, the detection with ultrasonic transducers simplifies the operation of the whole NDT system keeping a good resolution in the range of millimeters. In this study, it is proposed to analyze the resulting ultrasonic waves by means of a high resolution volumetric signal processing procedure based on the synthetic aperture focusing technique. This technique has been validated in classical ultrasonic arrangement, and its performance is proposed to be analyzed in front of such hybrid NDT approach. The study is supported by experimental results with the aim of damage localization and defect reconstruction in a metallic part.

2. Two-dimensional scan and SAFT analysis

Synthetic Aperture Focusing Technique (SAFT) is based on the back-propagation theory which creates a virtual image of the object under study by focusing the recorded data of a 1-dimensional or 2-dimensional A-scan processes. The algorithm superimposes the relatively low resolution A-scan data at every point of the scanned area, creating a higher resolution focused image with a higher signal to noise ratio (SNR), that is referred to as the Synthetic Aperture (SA) [9,10]. Depending on the implemented setup, the analysis can be performed in the time domain or in the frequency domain. SAFT technique can be used to generate a 2-dimensional image of a particular plane of the object or can be generalized to the 3-dimensional mode to cover all planes in the volume of the object. In the 3-dimensional mode, the reconstructed image can project maps of the defect in any plane, regardless of the plane used for the scan. This is a very flexible property that allows the scanning of the sample at any angle or plane, making the method more appropriate from the applicability point of view, since in general, the position and size of the defect that wants to be reconstructed is not known. In the time domain analysis, the Time Of Flight (TOF) is calculated across all SA points, starting from the source position at a particular scan point to all geometrical target points in the object's volume and back to the signal receiver at each particular scan point. For each geometrical point, an integration of all received signals at a particular value of TOF is calculated, to produce the final pixel value of this particular scan point in the final image. This integration of the signal at each pixel results in a higher contrast, resolution and better SNR value. The basic description of the SAFT algorithm is shown in figure 1, assuming a 3D object under inspection by a transmitter-receiver set in a pitch-catch mode.

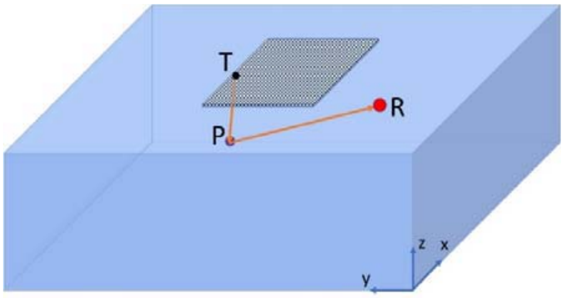

Figure 1. Geometry of the SAFT algorithm processing procedure, including the transmitter (T), the receiver (R), and the point of interest in the object's volume (P).

The TOF of the ultrasonic signal generated by a transmitted, *T*, and detected by a receiver, *R*, after it has been propagated to and reflected by an arbitrary point in the object volume, P, can be estimated following equation (1).

$$TOF_{(i,j,k)P} = \frac{|\vec{d}_{(i,j,k)P} - \vec{d}_{(i,j,z)T}| + |\vec{d}_{(i,j,k)P} - \vec{d}_{(i,j,z)R}|}{c} \quad (1)$$

where the *TOF* is the time of flight corresponding to the point *P,* and *d* is the displacement vector at positions of *T* ,*R* and *P*, while *i, j* and *k* represent the indexes of the volume image points in the *x*, *y*, *z* planes, respectively. The parameter *c* denotes the speed of the longitudinal waves in the material of the object [9–11]. This is done for every point in the A-scan measurements to produce a preliminary unfocused image y_R of the particular point *P*. The combination of all the individual images results into a high resolution focused image y_f . It is assumed that the scan is done at *M***N* points denoting a number of 2-dimensional transmitter steps, and also, only one receiver collects all the transmitted A-scan data from all transmitter scan points at an arbitrary point in the SA. Then, the final signal is given by equation (2).

$$y_f(P) = \sum_{j=1}^{N} \sum_{i=1}^{M} a(TOF_{(i,j)_P}, i, j) * y_R(TOF_{(i,j,k)_P}, i, j) \quad (2)$$

where y_R is the received signal at the $TOF_{(i,j,k)_P}$ at scan point indexes *i* and *j,* and y_f is the focused received signal from all the transmitter scan points at this particular receiver *R*. The $a(TOF_{(i,j)_P}, i, j)$ represents the weighting or apodization function [12]. For more than one receiver, we should modify equation (2) accordingly and consider the integration due to the scan of all receivers.

This derivation of the final image reconstruction using SAFT is only valid if the ultrasonic transmitter is considered as a point source which is completely applicable in the case of laser-generated ultrasonics. The receivers also need to be regarded as measuring data using a point-like transducer.

It should be noticed that, with regard to the part under inspection, the dimensions of the object should be large enough to avoid reflections on the object's boundaries, which could generate misleading data. The SAFT algorithm, the way it is described in the aforementioned analysis, can work with ultrasonic signals travelling at a single speed, if there is a composite structure that will result in different velocities of the sound inside each layer; the equation should be modified to consider each plane as a separate problem and combine all together at the end to generate the final image. Thus, the wave dispersion due to working in composite or inhomogeneous materials will result in violating the SAFT algorithm.

3. Experimental set-up

The experimental set-up is shown schematically in figure 2. A Nd:YAG laser is used emitting pulses of 8ns at a wavelength of 532nm and with 10mJ energy per pulse. The laser beam is directed towards a galvanometer that is programmed to scan a 2-dimensional area of the object's surface. The energy carried by the laser pulse is rapidly absorbed into a shallow volume of the material, and creates a localized thermo-elastic expansion inducing a stress wave that generates an acoustic pulse. For detection, we use two conventional Olympus Ultrasonic transducers, model V133-RM, with a 2.25 MHz central frequency, coupled to the surface of the object. Both sensors are placed on the laser beam incidence's surface, in a pitch-catch mode. The acquisition system is comprised of an Olympus preamplifier 5662, and a high-performance Gage A/D card model Oscar Express CSE4444, that allows a sampling frequency of 50 MHz at 16 bit of resolution. The recorded signals are filtered by a bandpass filter and added to an interpolation algorithm to remove the noise and low/high frequency components that are not of interest. We subtracted the background noise from the main signals and an averaging algorithm was performed to remove the DC components from the signal.

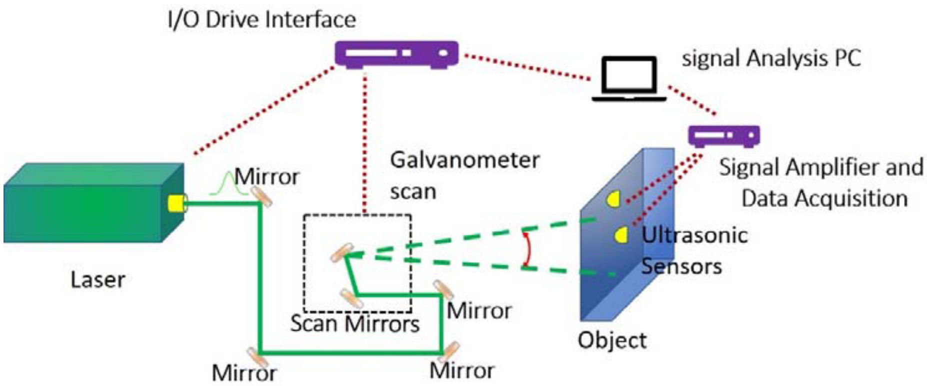

Figure 2. Schematic representation of the experimental set-up

Figure 3 shows the geometry of the 300mm x 200mm x 20mm aluminium sample considered in this study, having a cylindrical hole of 8mm diameter (the defect). Details about the scanning area and the sensors position are also shown in the figure.

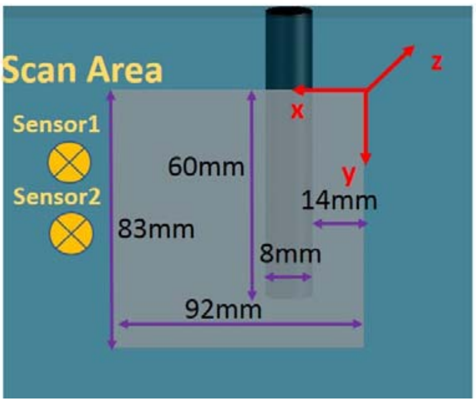

Figure 3. Aluminium sample with defect and the scan plane (in grey) for SAFT experiment.

The galvanometer shown in figure 2 is programmed to perform a 2-dimensional laser impact scan on the sample. As aforementioned, a 2-dimensional scan area of 92mm x 83mm is considered, resulting in 101 x 91 scan points corresponding to the *x* and *y* directions, respectively. The laser moves and impacts on each defined point of the object's surface, generating a broadband ultrasound signal. The experiment is done in a pitch-catch mode, where two receivers are placed at the positions indicated in figure 3. The programming and processing software for this experiment has been done using Matlab.

4. Experimental Results

Once the ultrasonic signals are collected, the SAFT algorithm is applied. The weighting function has been chosen to be a Gaussian shape. Thus, with the data obtained from the 2-dimensional laser scan on the sample and applying the signal pre-processing and the SAFT algorithm described above, the volumetric reconstruction of the defect under the scanned area is obtained as shown in figure 4. It must be noted that the volumetric representation considers only the reconstruction of the volume under the scan area. Also, it should be noted that commonly used SAFT described in the literature incorporates 1-dimensional line scanning instead of the 2-dimensional scanning area proposed in this study. In the classical case, only the reconstruction of one projection of the defect on one plane is possible. However, it is shown in this study that scanning on a 2-dimensional plane and integrating the SAFT algorithm over the object's volume of interest allow the defect visualization from different angles and at different depths, making possible a 3-dimensiona image reconstruction.

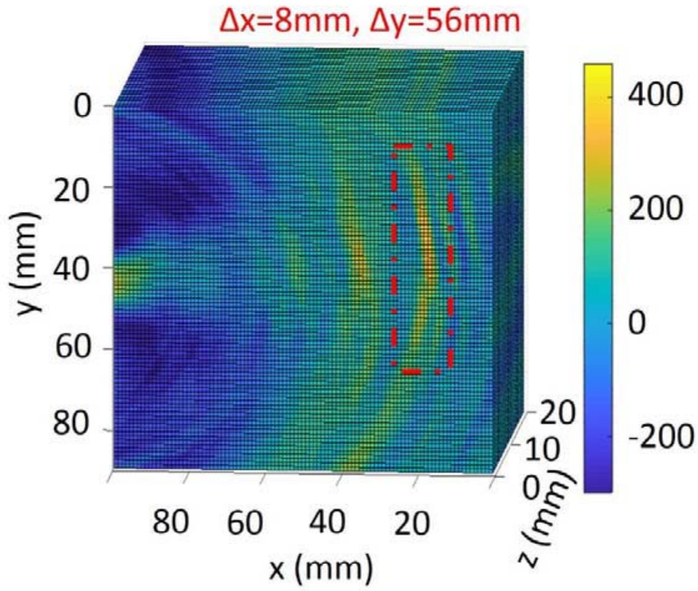

Figure 4: 3D slice for a full volume representation using a hybrid NDT approach and SAFT algorithm.

Figure 5 shows the contour map obtained as a projection on the *x*-*y* plane by grouping together all lines with a similar density level.

The contour map shows the reconstruction of the defect in the *x*-*y* plane: it is centred at x = 20mm, and y = 40mm with the corresponding size Δx = 8.2mm and Δy = 56mm. Compared with the actual size and position of the defect, the resulting reconstruction has the following errors: (Δx_{error} =2.5% and Δy_{error} = 6.7% and a positioning error of x_{error} = 2.5% and y_{error} = 22%.

It must be noticed that there are some shadows in the reconstruction of the defect that could be misleading. They come from the lower intensity back scattering and can be identified on the contour map.

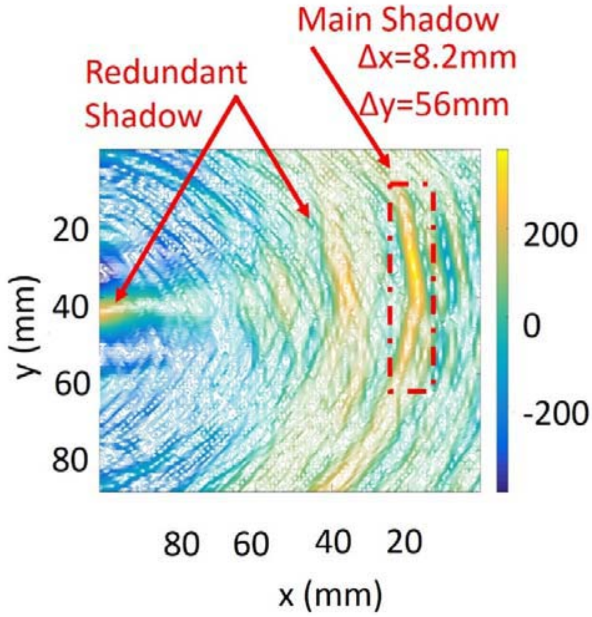

Figure 5: Contour map of the defect at *x*-*y* plane at z = 10mm using SAFT algorithm.

These shadows, as well as the resolution, are conditioned by some aspects of our experiment. On the one hand, the z-dimension of the object studied here was small compared with the x and y ones, which results in multiple reflections from the z boundaries, especially when the laser and the sensors are relatively far from the object. To solve this problem, the z dimension of the object under test should be large enough to avoid internal reflections from boundaries. This applies to all object boundaries in all directions. On the other hand, the position of the receiving sensors in the experiment was kept fixed and it only scanned the laser impact points. This configuration increased the angle between the excitation point and the position of the detected reflection by the ultrasonic sensor. Large angles reduce the performance of the SAFT algorithm and can significantly reduce the signal to noise ratio. These constraints can be resolved by increasing the object's depth and reducing the angle by scanning the receivers along with the laser beam.

5. Conclusion

The SAFT algorithm application, combined with a hybrid NDT approach composed by laser induced ultrasonic and conventional transducer receivers, has been studied. The results of the SAFT algorithm indicate the position and size of the defect, with the advantage of visualizing the defect in 3D. The projections of the SAFT planes make it easier to distinguish the location of the defect.

The defect position and size are determined with a relatively good signal to noise ratio, taking into consideration the limitations of the dimensions considered in the component under test. This means that the SAFT algorithm can give relatively good and reliable results even if the input signal and experimental conditions are not optimal.

Finally, two fixed ultrasonic receivers were used and they showed that by increasing the number of transmitters (i.e. laser scan points), the same good-quality images with a very limited number of receivers fixed at particular points can be obtained.

Future research involves more enhanced experimental conditions with better automated scan in both transmitted and received signals as well as the object's dimensions that satisfy the SAFT algorithm constraints.

Acknowledgements
Authors acknowledge the support of Ministerio de Economía y Competitividad with the Coordinated Project 'Light and sound waves in crystals, structured media and metamaterials', Ministerio de Economía e Innovación and European Union FEDER with the Project FIS2015-65998-C2-1 and FIS2015-65998-C2-2 and Conselleria d'Educación, Cultura y Deporte de la Generalitat Valenciana with the Project No. AICO/2016/060.

References
[1] Ham S, Song H, Oelze M L and Popovics J S 2017 A contactless ultrasonic surface wave approach to characterize distributed cracking damage in concrete *Ultrasonics* **75** 46–57
[2] Amjad U, Yadav S K and Kundu T 2015 Detection and quantification of pipe damage from change in time of flight and phase *Ultrasonics* **62** 223–36
[3] Kharrat M and Gaillet L 2015 Non-destructive evaluation of anchorage zones by ultrasonics techniques *Ultrasonics* **61** 52–61
[4] Masserey B, Raemy C and Fromme P 2014 High-frequency guided ultrasonic waves for hidden defect detection in multi-layered aircraft structures *Ultrasonics*
[5] Kreis T 2016 Application of Digital Holography for Nondestructive Testing and Metrology: A Review *IEEE Trans. Ind. Informatics* **12** 240–7
[6] Zhang K, Zhou Z and Zhou J 2015 Application of laser ultrasonic method for on-line monitoring of friction stir spot welding process. *Appl. Opt.* **54** 7483–9
[7] Brown M D, Allen T J, Cox B T and Treeby B E 2014 Control of optically generated ultrasound fields using binary amplitude holograms *IEEE International Ultrasonics Symposium, IUS* pp 1037–40
[8] Jen C and Wu K 2008 NDE using laser generated ultrasound and integrated ultrasonic transducer receivers *Ultrason. Symp.* 1516–9
[9] Spies M, Rieder H, Dillhöfer A, Schmitz V and Müller W 2012 Synthetic Aperture Focusing and Time-of-Flight Diffraction Ultrasonic Imaging — Past and Present 310–23
[10] Boonsang S, Zainal J and Dewhurst R J 2004 Synthetic aperture focusing techniques in time and frequency domains for photoacoustic imaging *Insight Non-Destructive Test. Cond. Monit.* **46** 196–9
[11] Stepinski T 2010 Synthetic aperture focusing techniques for ultrasonic imaging of solid objects *Synth. Aperture Radar* 438–41
[12] Jensen J A, Nikolov S I, Gammelmark K L and Pedersen M H 2006 Synthetic aperture ultrasound imaging *Ultrasonics* **44**